ISSN 0023-1584, Kinetics and Catalysis, 2011, Vol. 52, No. 2, pp. 242–250. © Pleiades Publishing, Ltd., 2011.
Original Russian Text © N.D. Golubeva, B.K. Dyusenalin, B.S. Selenova, S.I. Pomogailo, A.K. Zharmagambetova, G.I. Dzhardimalieva, A.D. Pomogailo, 2011, published in Kinetika i Kataliz, 2011, Vol. 52, No. 2, pp. 250–258.

Hybrid Polymer-Immobilized Palladium Nanoparticles: Preparation and Catalytic Properties[1]

N. D. Golubeva[a], B. K. Dyusenalin[b], B. S. Selenova[b], S. I. Pomogailo[a], A. K. Zharmagambetova[b], G. I. Dzhardimalieva[a], and A. D. Pomogailo[a]

[a] *Institute of Problems of Chemical Physics, Russian Academy of Sciences, Chernogolovka, Moscow oblast, 142432 Russia*
[b] *Sokol'skii Institute of Organic Catalysis and Electrochemistry, Academy of Sciences of Kazakhstan, Almaty, Kazakhstan*
e-mail: dzhardim@icp.ac.ru, adpomog@icp.ac.ru

Received June 8, 2010

Abstract—A new approach to the synthesis of mixed-type immobilized catalysts was developed: the frontal polymerization of a metal-containing monomer in the presence of a highly dispersed mineral support. The synthesis of an acrylamide complex of Pd(II) nitrate on the surface of SiO_2, Al_2O_3, or C and its subsequent polymerization and reduction resulted in the formation of an organic–inorganic composite that included nanosized Pd particles stabilized by a polymer matrix and an inorganic support. The resulting hybrid nanocomposites are efficient and selective catalysts for the hydrogenation reactions of cyclohexene and alkene and acetylene alcohols.

DOI: 10.1134/S0023158411020078

INTRODUCTION

Materials containing nanometer-sized metal particles exhibit unique physicochemical properties, and they have been intensively studied in the last few years [2]. The use of these materials as catalysts is of particular interest because the fraction of surface atoms with respect to the total number of atoms in a particle is very high in these systems, and they catalytic properties can be controlled by varying the sizes of nanoparticles [3–5]. Zerovalent palladium complexes and nanoparticles are widely known as efficient and selective catalysts for many organic reactions, for example, alkene arylation [6, 7], cross coupling [8], and the hydrogenation of dienes, olefins [9, 10], and unsaturated alcohols [11]. The main problem consists in the aggregative instability of metal nanoparticles and their tendency to agglomeration. Therefore, nanoparticles are immobilized on support surfaces (metal oxides, zeolites, carbon, etc.) or stabilized by introducing ligands, including polymers of various types.

A promising method for the preparation of metal polymers is polymer-mediated synthesis based on the thermal poly- and copolymerization of metal-containing monomers followed by the controlled thermolysis of the resulting products. This makes it possible to in situ form metal nanoparticles and a stabilizing polymer shell in a single step [12, 13]. The aim of this work was to prepare polymer-immobilized Pd nanoparticles in the presence of an inorganic support by the frontal polymerization of an acrylamide complex of Pd(II) nitrate and to evaluate their catalytic properties in the hydrogenation reactions of unsaturated compounds. This procedure is a new approach to the design of catalysts.

EXPERIMENTAL

Chemicals

Benzene and diethyl ether (chemically pure) were purified in accordance with standard procedures. Methanol (chemically pure), $PdCl_2 \cdot 4H_2O$ (chemically pure), acrylamide (AAm) (99.0%; Fluka), and toluene (chemically pure) were used without additional purification. Allyl alcohol (analytical grade; 99%) from Reanal (Budapest) was distilled at atmospheric pressure, and the main fraction with bp 96°C was collected. The acetylene alcohol 3,7,11,15-tetramethylhexadec-1-yn-3-ol (C_{20}) of chemically pure grade was purified by double distillation, and its purity was monitored by chromatography. Concentrated HNO_3 ($\rho = 1.18$ g/cm^3) was distilled at atmospheric pressure, and the main fraction with bp 110°C was taken. Silica gel 60 from Lancaster (220–240 mesh; specific surface area $S_{sp} = 240$ m^2/g) and preactivated (by vacuum calcination at 450°C) soot ($S_{sp} = 850$ m^2/g) and Al_2O_3 ($S_{sp} = 123$ m^2/g) were used as inorganic supports.

Preparation of $Pd(NO_3)_2 \cdot 2H_2O$

The synthesis of Pd(II) nitrate was performed by the interaction of freshly distilled concentrated nitric acid with freshly precipitated palladium hydroxide

---

[1] Communication no. 67 from the series *Reactivity of Metal-Containing Monomers*. For communication no. 66, see [1].

(2.6 g, 1.84×10^{-2} mol), which was prepared by the treatment of the complex salt Na_2PdCl_4 (5.5 g, 1.84×10^{-2} mol) with sodium hydroxide.

For $Pd(NO_3)_2 \cdot 2H_2O$ anal. calcd. (%): N, 10.5; H, 1.5; Pd, 39.9.

Found (%): N, 10.2; H, 1.4; Pd, 40.4.

IR spectrum of $Pd(NO_3)_2 \cdot 2H_2O$ (KBr pellet) (cm^{-1}): 850, 1386 (NO_3), 1650.

XPS (eV): Pd $3d_{5/2}$, 338.8; N $1s$, 407.2; O $1s$, 532.8.

Preparation of $Pd(CH_2{=}CHCONH_2)_2(NO_3)_2$ (PdAAm)

For the synthesis of PdAAm, we used a modified procedure for the preparation of the acrylamide complexes of transition metal nitrates [14]. Palladium(II) nitrate and acrylamide were mixed in a molar ratio of 1 : 5 in an inert atmosphere and ground to a paste-like state; then, the mixture was washed with dry ether and dried in a vacuum to constant weight.

For PdAAm anal. calcd. (%): C, 19.4; N, 15.0; H, 2.7; Pd, 28.6.

Found (%): C, 20.1; N, 15.1; H, 3.5; Pd, 29.4.

IR spectrum (KBr pellet) (cm^{-1}): 3190 (NH, ν_s), 3428 (NH, ν_{as}), 1665 (C=O), 1384 (NO_3).

Preparation of PdAAm on Inorganic Supports

The synthesis of PdAAm in the presence of SiO_2, Al_2O_3, and C was performed in accordance with the above procedure based on a 5–10 wt % Pd concentration in a mixed-type polymer + support catalyst. A mixture of the calculated amounts of Pd(II) nitrate, acrylamide, and SiO_2 (or Al_2O_3 or C) was ground in an agate mortar in a box with an inert atmosphere to a paste-like state, washed with benzene and ether, and dried in a vacuum at 30°C for no shorter than 12 h. The concentrations of Pd, wt %: 5.2 (PdAAm/SiO_2), 8.9 (PdAAm/Al_2O_3), and 10.2 (PdAAm/C).

Preparation of Pd/C

The traditional Pd/C catalyst was prepared by the impregnation of AG-3M activated carbon (S = 500 m^2/g) with an aqueous solution of H_2PdCl_4, which was prepared by boiling a mixture of palladium chloride, water, and concentrated hydrochloric acid for 2 h followed by reduction with $NaBH_4$ at 40°C and additional heating at 80°C for 15 min. Then, the catalyst was filtered off, washed with distilled water, and dried at 110°C for 3–5 h. The Pd content was 5 wt %.

Frontal Polymerization of PdAAm and PdAAm on Inorganic Supports

To perform frontal polymerization, the samples of PdAAm or PdAAm on a support were pressed as pellets 0.5–0.8 cm in diameter and 1.2–1.5 cm in height with a density of 1.45 ± 0.02 g/cm^3 and placed in a glass ampoule. To initiate polymerization, the bottom part of the ampoule with the sample was immersed at a depth of 0.2 cm in a bath with a heat carrier (Wood alloy) at 80–100°C. The rate of reaction was evaluated from the migration of the front of a colored zone. Powdered polymer and hybrid nanocomposite products were washed with methanol and ether and dried in a vacuum at room temperature to constant weight.

Hydrogenation of Cyclohexene and Unsaturated Alcohols

The experiments were performed in a glass batch reactor as a long-necked flask using isopropanol as a solvent at a cyclohexene concentration from 4.72×10^{-3} to 14.5×10^{-3} mol/l, a constant atmospheric pressure of hydrogen, and a temperature of 20°C under conditions of intense stirring (300–400 shaking per minute). The catalyst sample weight varied from 0.06 to 0.12 g. Hydrogen was supplied to the reactor from a calibrated receiver with a water lock. Before introducing cyclohexene, the catalyst was treated with hydrogen for 15 min immediately in the reactor with stirring. The rate of reaction was calculated graphically from the slope of the initial portions of the kinetic curves of hydrogen consumption. In parallel experiments, the discrepancy was no higher than 5%.

The hydrogenation of allyl and acetylene alcohols was performed in a glass batch reactor using ethanol as a solvent (20 ml) at a substrate concentration of 2.2×10^{-3} mol/l, a constant atmospheric pressure of hydrogen, and a temperature of 40°C under conditions of intense stirring (600–700 shaking per minute). The catalyst sample weight was 0.03 g. Hydrogen was supplied to the reactor from a gas meter, which was connected to an adapted calibrated receiver with a water lock. The catalyst was preliminarily treated with hydrogen for 30 min immediately in the reactor with intense stirring; then, a substrate was introduced into the reactor. The selectivity of the catalyst was evaluated as the fraction of the target product among all of the reaction products at a specified degree of conversion.

Analysis for Allyl Alcohol and Its Hydrogenation and Isomerization Products

The analysis was performed on a Kristall 2000M chromatograph with a flame-ionization detector under isothermal conditions using a multipurpose copper capillary column for organic compounds 50 m in length and 0.20 mm in an inner diameter. The column temperature was 90°C, and the injector chamber temperature was 180°C; helium served as a carrier gas; the injected sample volume was 0.2 μl. The samples of a liquid reaction mixture were taken two or three times in the course of an experiment with the use of a sampler.

Table 1. Elemental composition of the acrylamide complexes of Pd(II) nitrate and relative concentrations of various elements in them according to XPS data

Complex	Elemental composition, wt % (found/calculated)				Relative concentration, at %			
	C	H	N	Pd	C	O	N	Pd
$Pd(NO_3)_2$	–	1.4/1.5	10.2/10.5	40.4/39.9	–	68	21	10.5
PdAAm	20.1/19.4	3.5/2.7	15.1/15.0	29.4/28.6	52	27	19	2
$PdAAm/SiO_2$	–	–	–	5.2	16	57	6	0.7
PdAAm/C	–	–	–	10.2	83	14	2.8	0.2

Analysis of Catalysts

The elemental composition of samples was determined by organic microanalysis and flameless atomic absorption spectrometry on a Saturn instrument. The X-ray diffraction of powders was studied on DRON UM-2 and Philips PW 1050 diffractometers using CuK_α radiation ($\lambda = 1.54184$ Å). The IR absorption spectra were measured on a Specord 75 IR spectrophotometer; the samples were pressed as pellets with KBr.

An ES-2401 spectrometer with a magnesium anode was used to obtain XPS spectra. The X-ray tube power was 200 W; the pressure in the analyzer chamber was 10^{-6} Pa, and the analyzer energy was 50 eV. The spectrometer was calibrated using the Au $4f_{7/2}$ line (84 eV). The binding energy (BE) corresponding to the C 1*s* electron line in an alkyl group was taken equal to 285.0 eV. The BE determination accuracy was 0.1–0.2 eV.

The electron-microscopic studies were performed on a JEOL transmission electron microscope (TEM) with an accelerating voltage of 100 kV.

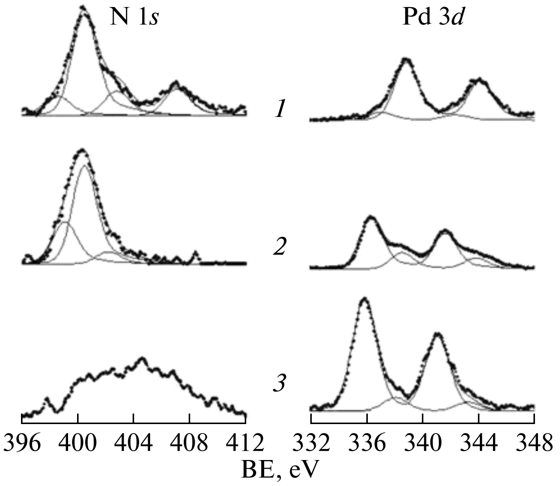

Fig. 1. XPS spectra of (*1*) acrylamide complex monomer with $Pd(NO_3)_2$, (*2*) PdAAm after polymerization, and (*3*) the same after cyclohexene hydrogenation.

The specific surface areas of inorganic supports and polymer hybrid compositions and the pose sizes were determined from nitrogen adsorption at 77 K by a volumetric method using an AUTOSORB-1 instrument (Quantachrome, United States).

RESULTS AND DISCUSSION

Synthesis of $Pd(CH_2{=}CHCONH_2)(NO_3)_2$ (PdAAm)

The acrylamide complex of Pd(II) nitrate was synthesized by the replacement of crystal water in the metal nitrate crystal hydrate by acrylamide molecules. Table 1 summarizes the results of the elemental analysis and spectroscopic characteristics of the resulting complex.

The IR-spectroscopic data suggest that the metal atom was coordinated through the oxygen atoms of the carbonyl group of the AAm ligand: the bands of CO vibrations (1665 cm^{-1}) were shifted to the long-wavelength region, as in analogous transition metal complexes [15]. This was supported by shifts in the C 1*s* (BE = 288.3 eV), N 1*s* (BE = 399.8 eV), and O 1*s* (BE = 531.6 eV) lines in XPS spectra toward the high-energy region by 0.5, 0.7, and 0.5 eV, respectively. Bands due to the stretching vibrations of the nitrate ion at 1384 cm^{-1} (NO_3) were also detected in the IR spectra of complexes. The presence of a low-intensity line with BE = 337.2 eV in the Pd $3d_{5/2}$ XPS spectrum and an increase in the intensity of a line with BE = 285.7 eV may be explained by additional π coordination of the metal atom with respect to the double bond of the ligand. Such examples frequently occur in the case of Pd alkene complexes [16]. In the surface layer, the Pd/N and O/N atomic ratios are 0.11 and 1.4, respectively (Table 1), and the intensity of a line with BE = 407.2 eV in the N 1*s* spectrum is 10% of the integrated intensity of the entire spectrum. This observation quantitatively correlates with the intensity of a line with BE = 338.8 eV in the Pd $3d_{5/2}$ spectrum (Fig. 1) and suggests the shielding of Pd atoms by AAm groups.

Frontal Polymerization of PdAAm in the Absence and Presence of an Inorganic Support

As found previously [15, 17], the acrylamide complexes of metal nitrates can effectively undergo polymerization in a condensed state in the frontal mode, that is, under conditions when monomer conversion into a polymer begins in a local reaction zone and layer-by-layer propagates over the entire volume. The reaction occurs under the mildest conditions known for processes of this kind, namely, at atmospheric pressure and thermal initiation (without the use of chemical initiators and activators). Under conditions of the steady-state propagation of a thermal wave, polymerization occurs in a narrow temperature range. The heat released in the reaction zone is transferred to the heating zone, where the substance is heated because of thermal conductivity; the temperature increases to a value at which the reaction comes into play; that is, the propagation of a polymerization front occurs. The reaction is initiated by the generation of a short-time (~15 s) thermal agitation ("ignition") at the end portion of a glass ampoule, where the sample of PdAAm monomer or its mixture with a mineral filler pressed as a cylinder is placed. In this case, the appearance and propagation of a melting zone (first-order phase transition) and a color change from light brown to dark brown and black are observed (the rate of reaction is monitored using the migration of the boundary of this zone). Kinetic studies suggest the high rate of frontal polymerization of the acrylamide complex of Pd(II) (w = 0.038 cm/s), the ignition temperature of which (80–100°C) is much lower than the corresponding characteristics of AAm complexes with the nitrates of Co(II), Ni(II), etc. (170–180°C) [15].

At higher ignition temperatures (150–170°C), the ejection of reaction mass from the glass tube and a change to the combustion mode (!) were observed; this was likely due to the formation of highly dispersed pyrophoric palladium particles. According to XPS data, the main line in the Pd $3d_{5/2}$ spectrum of the polymerization product corresponded to BE = 336.5 eV, which is higher than BE in Pd^0 (<336.0 eV). This can be explained by the formation of highly dispersed Pd^0 and $Pd^{\delta+}$ particles [10, 18]. It is likely that an increase in the BE of the main line in the N 1s spectrum to 401.7 eV was due to the occurrence of polymer chain cyclization reactions with the formation of imide groups [19].

The previously developed approach to the preparation of nanocomposite materials using frontal polymerization [20] is of interest for the development of polymer-immobilized catalysts of the mixed (hybrid) metal nanoparticles–polymer–inorganic support type. Indeed, the preparation of an acrylamide complex of Pd(II) on the surface of a mineral support and its subsequent polymerization resulted in the formation of a polymer–inorganic composite. According to electron-microscopic data, this composite consisted of nanosized Pd particles 4–8 nm in diameter and their aggregates of size 10–20 nm stabilized by a polymer matrix (Fig. 2).

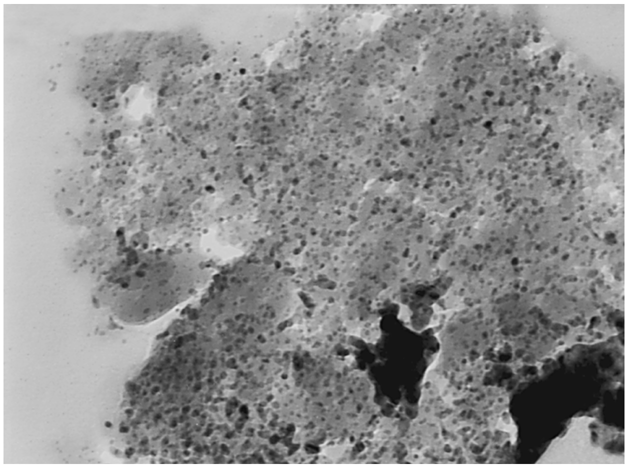

Fig. 2. Electron micrograph of poly-PdAAm/SiO_2 (magnification of 125000×).

As was expected, the action of fillers (SiO_2, Al_2O_3, and C) on the autowave polymerization mode (w = 0.024 cm/s) manifested itself as the fact that the polymerization front acquired signs of spatiotemporal stabilization, which, what is more important, was also reached at high degrees of filling (75 wt %).

The X-ray diffraction patterns of the resulting samples exhibited broad diffraction peaks in a 2θ range from 36° to 85°, which correspond to crystalline Pd^0 (Fig. 3). Diffuse diffraction peaks and broadened lines suggest an ultradisperse state of particles (Table 2). The resulting nanocomposites typically have a microporous structure with a pore size of several nanometers to 20 nm and a uniform pore size distribution (Fig. 4). Note the fact that the specific surface area of mixed-type supports decreased after the frontal polymerization of PdAAm on their surfaces, although it was greater than S_{sp} of the PdAAm polymerization product in the absence of an inorganic support (Table 3). Thus, the resulting hybrid nanocomposites had a sufficiently developed surface and pore structure to provide the accessibility of the active centers of a catalyst to

Table 2. Results of the XPS, XRD, and TEM analysis of polymer hybrid nanocomposites based on PdAAm

Nanocomposite	Pd $3d_{5/2}$ XPS spectrum, eV	Particle size of Pd, nm
PdAAm	336.5, 338.9	3.9
PdAAm/SiO_2	337.6, 338.9	3.6–4.0
PdAAm/Al_2O_3	–	4
PdAAm/C	338.5, 341.3	8

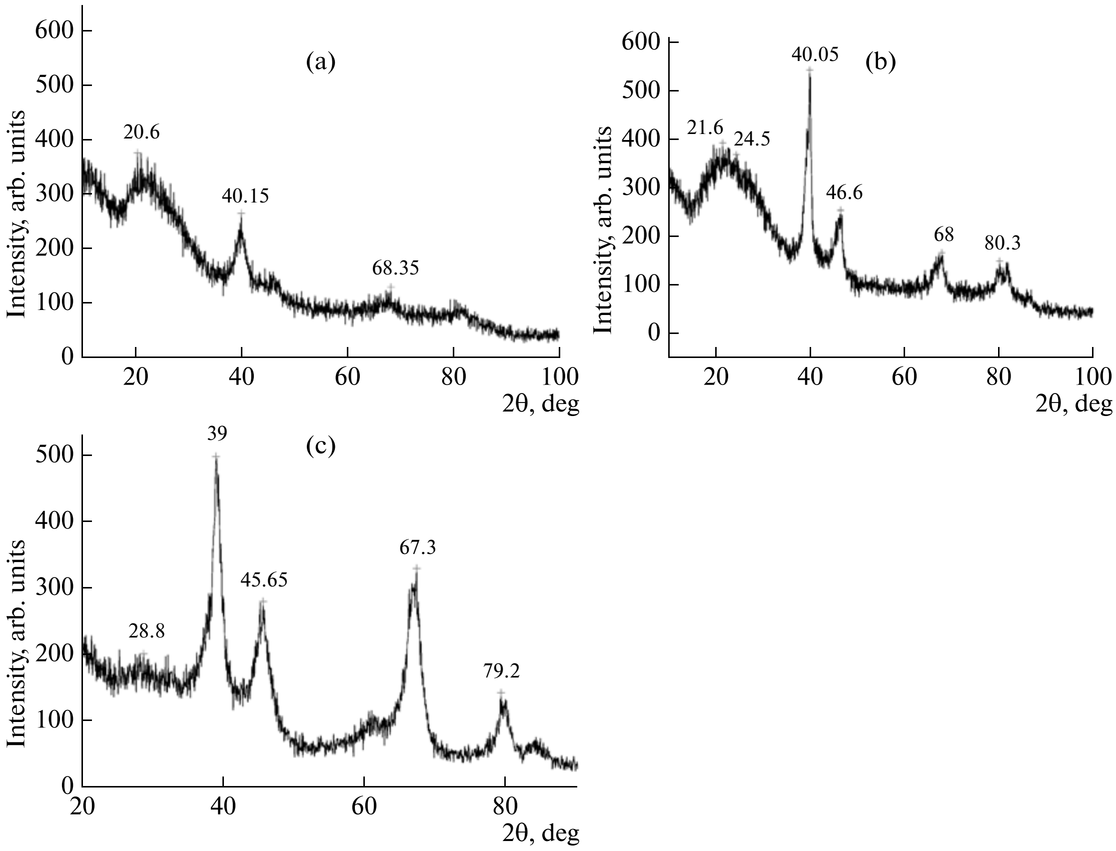

Fig. 3. Diffraction patterns of PdAAm/SiO_2 samples prepared at (a) 115 and (b) 130°C and (c) a PdAAm/Al_2O_3 sample.

reagents and their high activity in the test catalytic reactions.

Catalytic Properties of the PdAAm on Inorganic Supports in the Reaction of Cyclohexene Hydrogenation

The test systems exhibited a sufficiently high activity in the model reaction of cyclohexene hydrogenation. Thus, under comparable conditions, the initial rate of reaction on the poly-PdAAm/Al_2O_3 catalyst was higher by a factor of almost 2 than that on standard Pd/C (Table 4, Fig. 5).

Table 3. Specific surface areas and pore sizes for polymer hybrid nanocomposites based on PdAAm

Sample	S_{sp}, m^2/g	Pore volume, cm^3/g	Average pore radius, Å
poly-PdAAm	18.2	0.10	113.2
SiO_2	238.7	0.41	34.3
poly-PdAAm/SiO_2	146.8	0.28	37.8
Al_2O_3	123.6	–	–
poly-PdAAm/Al_2O_3	60.2	0.17	55.0

The test nanocomposites retained catalytic activity in repeatedly performed reaction cycles, and the occurrence of the nanocomposites in an immobilized form makes it possible to separate them from the reaction medium and to use them repeatedly; what is very important, intermediates formed on the catalyst can be studied using various physicochemical techniques. In some cases, even an increase in activity was observed in the repeated use; that is, the so-called development of a catalyst occurred, which is characteristic of many immobilized systems. In particular, this phenomenon was demonstrated recently using the polymer clusters of rhodium as an example [21].

The catalytic properties of the test composites are affected by the conditions of formation of Pd nanoparticles, for example, the use of various frontal polymerization conditions in an inert atmosphere or post-thermal treatment at 100–150°C in a reducing atmosphere of hydrogen (Fig. 6). Thus, as the temperature of the reductive treatment of nanocomposites was increased, the rate of cyclohexene hydrogenation on them decreased. Analogous behaviors were also observed in catalytic systems based on both SiO_2 and Al_2O_3 (Table 4). It is most likely that the reason for the decrease in the rate of reaction is the agglomeration of Pd particles at relatively high nanocomposite treatment temperatures.

Table 4. Initial rates of cyclohexene hydrogenation (w_0) in the presence of hybrid polymer-immobilized Pd nanoparticles

Sample	Preparation conditions	w_0, (mol H_2) (mol Pd)$^{-1}$ min^{-1}		
		cycle 1	cycle 2	cycle 3
poly-PdAAm/SiO_2	FP	22.9	16.7	–
	FP, 100°C	10.8	12.6	10.1
	FP, 120°C	13.4	10.50	11.2
	FP, 150°C	1.1	3.48	5.2
poly-PdAAm/Al_2O_3	FP	33.4	24.80	22.7
	FP, 100°C	11.3	9.90	–
	FP, 140°C	2.5	4.0	4.3
poly-PdAAm/C	FP	11.3	–	–
Pd/C		11.6	11.6	–

Note that, in poly-PdAAm after hydrogenation, the main fraction of Pd (90%) occurred in a zerovalent state (see Fig. 1) and its shielding by a polymer matrix decreased, as evidenced by an increase in the Pd content of the surface layer (from 1.5 at % in the starting polymer complex to 4.3 at %). The polymer matrix also underwent changes, which manifested themselves in a broadening of the N 1*s* spectrum.

Thus, the resulting hybrid polymer-immobilized Pd nanoparticles exhibited high activity in the reaction of cyclohexene hydrogenation and retained it in repeated cycles. The catalytic properties of nanocomposites depend on preparation conditions, which, evidently, affect the size of formed Pd nanoparticles.

Catalytic Properties of Poly-PdAAm Nanocomposites on SiO_2 and Al_2O_3 in the Hydrogenation of Allyl Alcohol

It is well known that substrate isomerization in the hydrogenation of allyl alcohol is an undesirable side reaction, which sometimes can even predominate over the main process. Therefore, isomerization should be suppressed to increase the yield of target products. In known examples, catalysts based on Pd nanoparticles encapsulated in polyelectrolyte multilayers [22] or dendrimers [23] were used for this purpose. The nanocomposites under consideration are active catalysts for the hydrogenation of ally alcohol. As evidenced by experimental data (Table 5), they exhibited different activities; however, both exhibited high selectivity in this case. The main product of the hydrogenation of allyl alcohol is 1-propanol; propionaldehyde (allyl alcohol isomerization product) was also identified in insignificant amounts (to 2% in the presence of poly-PdAAm/Al_2O_3 and to 5% in the presence of poly-PdAAm/SiO_2). Any other products were not detected. It is likely that a higher rate of reaction on PdAAm/SiO_2 was due to its more developed surface and specific features of substrate adsorption on this surface (see Table 3).

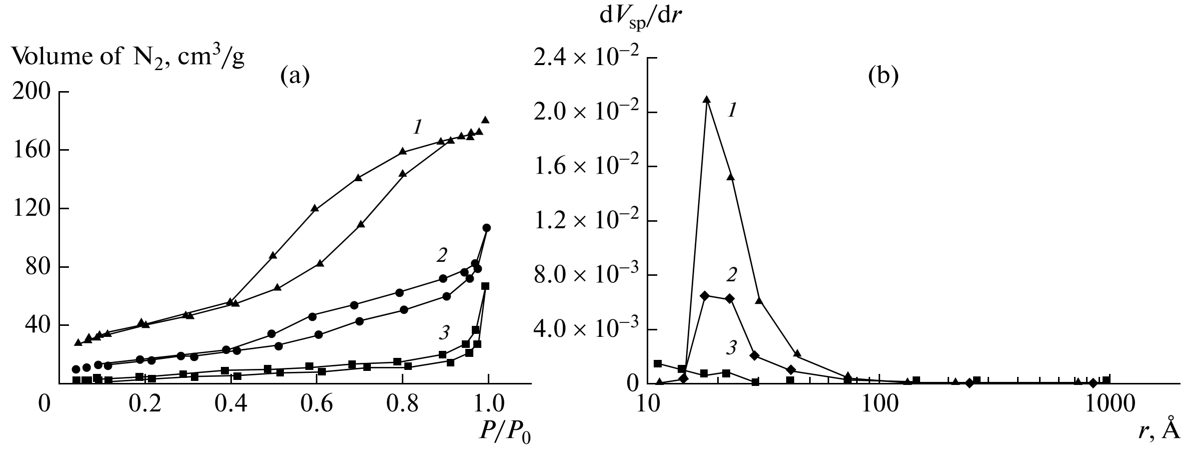

Fig. 4. (a) Nitrogen adsorption–desorption isotherms and (b) differential pore radius (r) distribution curves in polymer hybrid nanocomposites: (*1*) poly-PdAAm/SiO_2, (*2*) poly-PdAAm/Al_2O_3, and (*3*) poly-PdAAm.

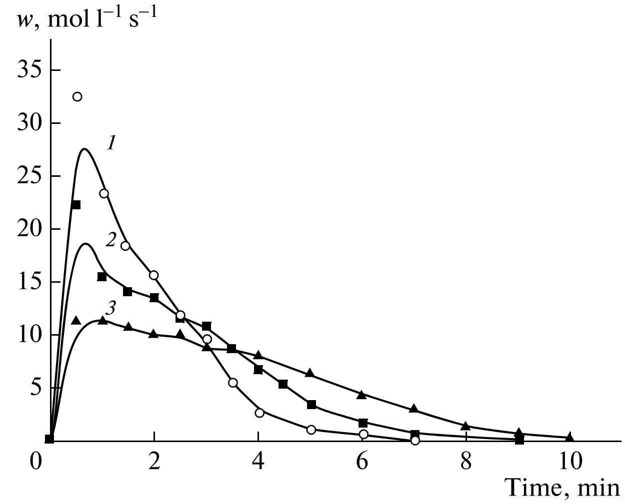

Fig. 5. Hydrogen uptake kinetics in cyclohexene hydrogenation in the presence of (*1*) poly-PdAAm/Al_2O_3, (*2*) poly-PdAAm/SiO_2, and (*3*) Pd/C. Catalyst sample weight, 0.05–0.10 g; temperature, 20°C; H_2 pressure, 0.1 MPa; solvent, isopropanol; and initial cyclohexene amount, 6.9 mmol.

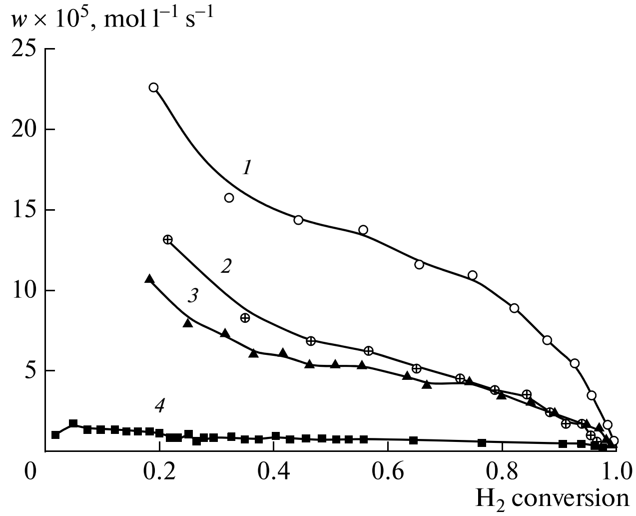

Fig. 6. Dependence of the rate of cyclohexene hydrogenation on the H_2 conversion in the presence of poly-PdAAm/SiO_2 samples prepared under various conditions: (*1*) frontal polymerization in a self-generated atmosphere, (*2*) frontal polymerization in a reductive atmosphere at 118–120°C, (*3*) the same at 104–106°C, and (*4*) the same at 150°C. Catalyst sample weight, 0.10 g; temperature, 20°C; H_2 pressure, 0.1 MPa; solvent, isopropanol; and initial cyclohexene amount, 6.9 mmol.

The stability of catalysts was evaluated by performing the consecutive cycles of allyl alcohol hydrogenation on the same sample (Fig. 7). The catalysts retained high activity in repeated cycles; this is especially characteristic of poly-PdAAm/SiO_2, the rate of reaction on which decreased only after the tenth cycle. It is likely that a pause of several hours (after sixth and ninth cycles) in the process facilitated the equalizing of the concentrations of all of the participants of the process (solvent, products, and substrate) near active sites, which resulted in an increase in the reaction rate.

Catalytic Properties of PdAAm Nanocomposites on SiO_2 and Al_2O_3 in 3,7,11,15-Tetramethylhexadec-1-yn-3-ol Hydrogenation

It is convenient to study steric effects on the selectivity of a catalytic reaction using the hydrogenation of a spatially hindered long-chain C_{20} acetylene alcohol as an example. The rate of its hydrogenation was much lower than that of allyl alcohol (Fig. 8, Table 5); this fact can be explained by diffusion limitations, which hinder the access of the reactant to the active sites of the catalyst.

As was found by chromatographic analysis, the triple bond of the C_{20} acetylene alcohol can be readily reduced to a double bond (Fig. 9). The maximum reaction rate was reached after 10 min (see Fig. 8); then, it dramatically decreased. In this time, the acetylene alcohol was almost completely converted into reaction products in the system with the participation of poly-PdAAm/SiO_2. However, the process was nonselective. Simultaneously with the hydrogenation of the triple bond, the reduction of the double bond occurred, so that both saturated 3,7,11,15-tetrameth-

Table 5. Initial rates of and selectivities of the hydrogenation of allyl alcohol and 3,7,11,15-tetramethylhexadec-1-yn-3-ol on Pd hybrid polymer-immobilized catalysts

Catalyst	Allyl alcohol		C_{20} acetylene alcohol	
	$w \times 10^5$, mol l^{-1} s^{-1}	selectivity, %	$w \times 10^5$, mol l^{-1} s^{-1} (after 10 min)	selectivity, %
poly-PdAAm/Al_2O_3	4.98	97.2	1.4	70
poly-PdAAm/SiO_2	56.7	95.6	2.8	49.9

Note: Reaction conditions: alcohol concentration, 0.225 mol/l; catalyst sample weight, 0.03 g (1.41 × 10^{-5} g-at Pd/g); temperature, 40°C; pressure, 0.1 MPa; solvent, 20 ml of ethanol.

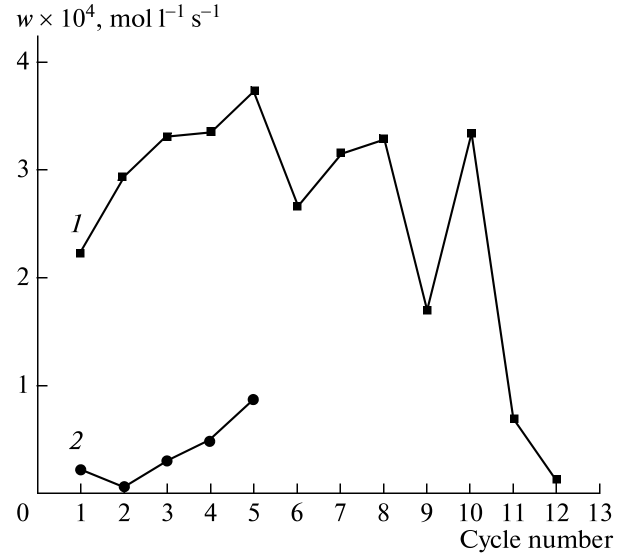

Fig. 7. Consecutive hydrogenation of allyl alcohol portions in the presence of (*1*) poly-PdAAm/SiO_2 and (*2*) poly-PdAAm/Al_2O_3. Initial substrate amount, 2.58 mmol; catalyst sample weight, 0.03 g; solvent, 20 ml of ethanol; and temperature, 40°C.

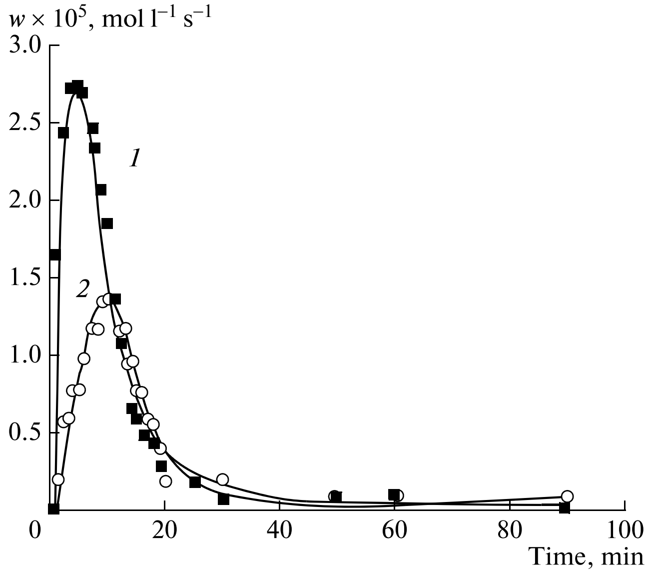

Fig. 8. Time variation of the rate of 3,7,11,15-tetramethylhexadec-1-yn-3-ol hydrogenation on immobilized (*1*) poly-PdAAm/SiO_2 and (*2*) poly-PdAAm/Al_2O_3 catalysts. Catalyst sample weight, 0.03 g; temperature, 40°C; H_2 pressure, 0.1 MPa; and solvent, 20 ml of ethanol.

ylhexadecan-1-3-ol and the corresponding olefin alcohol were detected among the reaction products.

A somewhat different behavior was observed upon the hydrogenation of the C_{20} acetylene alcohol in the presence of poly-PdAAm/Al_2O_3. Initially, it was mainly converted into the corresponding olefin alcohol and the concentration of the saturated alcohol was no higher than 8–10%. Only after 20 min when about 10% of the starting substrate remained in the reaction mixture, the intense hydrogenation of the double bond came into play with the formation of the aliphatic alcohol. The selectivity of olefin alcohol formation was 70% (Table 5). A comparison between Figs. 8 and 9 allowed us to conclude that the triple bond was rapidly reduced to the double bond and the formation of the saturated alcohol occurred very slowly ($w = 0.1 \times 10^{-5}$ mol l^{-1} s^{-1}); that is, the double bond was hydrogenated more slowly than the triple bond by a factor of 7–10. Currently, the mechanism of the selective action of the test hybrid polymer-immobilized catalysts remains incompletely known, and it, as well as catalytic process optimization, calls for further investigation.

Thus, we developed a procedure for the preparation of mixed-type polymer-immobilized Pd nanoparticles on the surface of supports. These nanoparticles are efficient and selective catalysts for the hydrogenation of unsaturated compounds. In the case of unsaturated alcohols, the hydrogenation reaction path predominates over isomerization. The test nanocomposites retained catalytic activity in repeated cycles. The circumstance that they occurred in an immobilized form facilitated their separation from the reaction medium and repeated use and made it possible to study the transformations of catalytic intermediates. The subsequent studies will be oriented to the detection of size effects (a study of the dependence of reaction rate and selectivity on the size of palladium nanoparticles) and

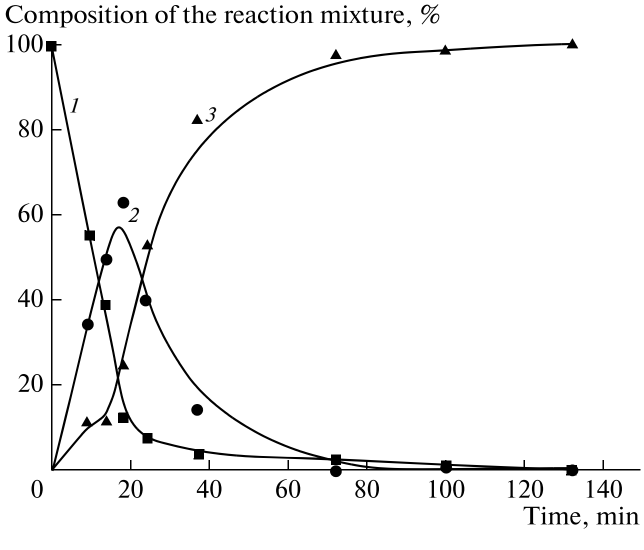

Fig. 9. Changes in the composition of the reaction mixture during 3,7,11,15-tetramethylhexadec-1-yn-3-ol hydrogenation in the presence of poly-PdAAm/SiO_2: (*1*) C_{20} acetylene alcohol, (*2*) the resulting ethylene alcohol, and (*3*) the resulting saturated alcohol. Catalyst sample weight, 0.03 g; temperature, 40°C; H_2 pressure, 0.1 MPa; and initial C_{20} content, 0.225 mol/l.

the use of nanocomposites based on other metals in hydrogenation reactions.

ACKNOWLEDGMENTS

We are grateful to Cand. Sci. (Chem.) A.M. Lyakhovich for the XPS analysis of the samples.

REFERENCES

1. Dzhardimalieva, G.I., Dorokhov, V.G., Golubeva, N.D., Pomogailo, S.I., Lyakhovich, A.M., Savchenko, V.I., and Pomogailo, A.D., *Izv. Akad. Nauk, Ser. Khim.*, 2009, no. 10, p. 2007.
2. Pomogailo, A.D. and Kestelman, V.N., *Metallopolymer Nanocomposites*, Heidelberg: Springer, 2005.
3. Pomogailo, A.D., *Kinet. Katal.*, 2004, vol. 45, p. 67 [*Kinet. Catal.* (Engl. Transl.), vol. 45, p. 61].
4. Wohrle, D. and Pomogailo, A.D., *Metal Complexes and Metals in Macromolecules*, Weinheim: Wiley-VCH, 2003.
5. Campelo, J.M., Luna, D., Luque, R., Marinas, J.M., and Romero, A.A., *ChemSusChem*, 2009, vol. 2, p. 18.
6. Heck, R.F., *Palladium Reagents in Organic Synthesis*, New York: Academic, 1985.
7. Andersson, C.M., Karabelas, K., and Hallberg, A., *J. Org. Chem.*, 1985, vol. 50, p. 3891.
8. Ogasawar, S. and Kato, S., *J. Am. Chem. Soc.*, 2010, vol. 132, p. 4608.
9. Hirai, M., Yakaru, N.I., Seta, Y., and Hodosima, S., *React. Funct. Polym.*, 1998, vol. 37, p. 121.
10. Belyi, A.A., Chigladze, L.G., Rusanov, A.L., Shalikiani, M.O., Tabidze, R.S., Gagarin, S.G., Shpiro, E.S., Antoshin, G.V., Minachev, Kh.M., and Vol'pin, M.E., *Izv. Akad. Nauk SSSR, Ser. Khim.*, 1987, no. 10, p. 2153.
11. Kidambi, S., Dai, J., Li, J., and Bruening, M.L., *J. Am. Chem. Soc.*, 2004, vol. 126, p. 2658.
12. Pomogailo, A.D., Dzhardimalieva, G.I., Rozenberg, A.S., and Muraviev, D.N., *J. Nanopart. Res.*, 2003, vol. 5, p. 497.
13. Dzhardimalieva, G.I., Pomogailo, A.D., Rozenberg, A.S., and Leonowicz, M., in *Magnetic Nanoparticles*, Gubin, S.P., Ed., Weinheim: Wiley-VCH, 2009.
14. Savost'yanov, V.S., Ponomarev, V.I., Pomogailo, A.D., Selenova, B.S., Ivleva, I.N., Starikov, A.G., and Atovmyan, L.O., *Izv. Akad. Nauk SSSR, Ser. Khim.*, 1990, vol. 39, p. 726 [*Bull. Acad. Sci. USSR, Div. Chem. Sci.* (Engl. Transl.), vol. 39. p. 674].
15. Pomogailo, A.D. and Dzhardimalieva, G.I., *Vysokomol. Soed., Ser. A*, 2004, vol. 46, p. 437 [*Polym. Sci., Ser. A: Polym. Phys.* (Engl. Transl.), vol. 46, p. 250].
16. Shi, T. and Elding, L.I., *Inorg. Chem.*, 1998, vol. 37, p. 5544.
17. Dzhardimalieva, G.I., Pomogailo, A.D., and Volpert, V.A., *J. Inorg. Organomet. Polym.*, 2002, vol. 12, p. 1.
18. Okitsu, K., Yue, A., Tunabe, S., and Matsumoto, H., *Bull. Chem. Soc. Jpn.*, 2002, vol. 75, p. 449.
19. Fortenberry, D.I. and Pojman, J.A., *J. Polym. Sci., Part A: Polym. Chem.*, 2000, vol. 38, p. 1129.
20. Barelko, V.V., Pomogailo, A.D., Dzhardimalieva, G.I., Evstratova, S.I., Rozenberg, A.S., and Uflyand, I.E., *Chaos*, 1999, vol. 9, p. 342.
21. Pomogailo, S.I., Dorokhov, V.G., Lyakhovich, A.M., Mikhailova, S.S., Dzhardimalieva, G.I., and Pomogailo, A.D., *Kinet. Katal.*, 2006, vol. 47, p. 742 [*Kinet. Catal.* (Engl. Transl.), vol. 47, p. 719].
22. Kidambi, S., Dai, J., Li, J., and Bruening, M.L., *J. Am. Chem. Soc.*, 2004, vol. 126, p. 2658.
23. Jiang, Y. and Gao, Q., *J. Am. Chem. Soc.*, 2006, vol. 128, p. 716.